Sooryanarayana Varambally ORCID iD: 0000-0002-2277-1127

Characterization of Glycine-N-Acyltransferase Like 1 (GLYATL1) in prostate cancer

Marie-Lisa Eich[1], Darshan Shimoga Chandrashekar[1], Maria Del Carmen Rodriguez Peña[1], Alyncia D. Robinson[1], Javed Siddiqui[3], Stephanie Daignault-Newton[4], Balabhadrapatruni V. S. K. Chakravarthi[1], Lakshmi Priya Kunju[3], George J. Netto[1*], Sooryanarayana Varambally [1,2*]

[1] Department of Pathology, The University of Alabama at Birmingham, Birmingham, AL, USA

[2] O'Neal Comprehensive Cancer Center, University of Alabama at Birmingham

[3] Department of Pathology, The University of Michigan, Ann Arbor, MI, USA

[4]Department of Biostatistics, The University of Michigan, Ann Arbor, MI, USA

Running Title: Characterization of GLYATL1 in prostate cancer.

Corresponding Authors: Sooryanarayana Varambally, Department of Pathology, The University of Alabama at Birmingham, WTI Building, Suite l, Birmingham, AL 35249-7331. Email: svarambally@uabmc.edu

and

George J. Netto, Professor and Chair, Department of Pathology, The University of Alabama at Birmingham, WP Building, Suite P230 l 619 19th Street, South, Birmingham, AL 35249-7331. Phone: (205) 934-0014. Email: gnetto@uabmc.edu

Keywords: Prostate cancer, GLYATL1, immunohistochemistry, Androgen, ETV1

Competing interests: None.

Funding/support: UAB O'Neal Comprehensive Cancer Center Development Fund

Abstract

Background

Recent microarray and sequencing studies of prostate cancer showed multiple molecular alterations during cancer progression. It is critical to evaluate these molecular changes to identify new biomarkers and targets. We performed analysis of Glycine-N-Acyltransferase Like 1 (GLYATL1) expression in various stages of prostate cancer in this study and evaluated the regulation of GLYATL1 by androgen.

Method

We performed *in silico* analysis of cancer gene expression profiling and transcriptome sequencing to evaluate GLYATL1 expression in prostate cancer. Furthermore, we performed immunohistochemistry using specific GLYATL1 antibody using high density prostate cancer tissue microarray containing primary and metastatic prostate cancer. We also tested the regulation of GLYATL1 expression by androgen and ETS transcription factor ETV1.In addition, we performed RNA-sequencing of GLYATL1 modulated prostate cancer cells to evaluate the gene expression and changes in molecular pathways.

Results

Our *in silico* analysis of cancer gene expression profiling and transcriptome sequencing we revealed an overexpression of GLYATL1 in primary prostate cancer. Confirming these findings by immunohistochemistry, we show that GLYATL1 is overexpressed in

primary prostate cancer compared to metastatic prostate cancer and benign prostatic tissue. Low grade cancers had higher GLYATL1 expression compared to high grade prostate tumors. Our studies showed that GLYATL1 is upregulated upon androgen treatment in LNCaP prostate cancer cells which harbors ETV1 gene rearrangement. Furthermore, ETV1 knockdown in LNCaP cells showed downregulation of GLYATL1 suggesting potential regulation of GLYATL1 by ETS transcription factor ETV1. Transcriptome sequencing using the GLYATL1 knockdown prostate cancer cell lines LNCaP showed regulation of multiple metabolic pathways.

Conclusions

In summary, our study characterizes the expression of GLYATL1 in prostate cancer and explores regulation of its regulation in prostate cancer showing role for androgen and ETS transcription factor ETV1. Future studies are needed to decipher the biological significance of these findings.

1. Introduction

Prostate cancer (PCa) is the most prevalent cancer entity in men with estimated 174,650 new cases in 2019 in the USA. Despite recent advances in diagnosis and treatment it remains the second most cancer-related cause of death.(1) Recent molecular studies have paved the way to a better understanding of the underlying biology of tumor growth and progression. This offers new possibilities to find new therapeutic targets for the disease. (2,3)

GLYATL1 encodes an enzyme that catalyzes arylacetyl transfer.(4,5) In non-cancerous tissue it was found to be highly expressed in liver and kidney, and to a lesser extent in

pancreas, testis, ovary and stomach.(6) Human Glycine N-acyltransferases (GLYATL, GLYATL1, GLYATL2, and GLYATL3) are involved in conjugation of carboxylic acids to glycine and glutamine. This conjugation is thought to be a part of a pathway for the detoxification of benzoate and other xenobiotics.(7) GLYAT plays a major role in liver metabolism. It regulates mitochondrial ATP production, glycine availability, CoASH (Coenzyme A) availability and the detoxification of various organic acids.(7-9) Human GLYATL2 conjugates medium- and long-chain saturated and unsaturated acyl-CoA esters to glycine producing N-oleoyl glycine and N-arachidonoyl glycine. The latter are structurally and functionally related to endocannabinoids and have been identified as signaling molecules that regulate functions such as perception of pain and body temperature. They have also been found to have anti-inflammatory properties.(10) Furthermore, GLYATL2 was found to be a target of ETS transcription factor ETV1, which is along with other ETS transcription factors rearranged in ~50% of human prostate cancer cases.(11,12)

Microarray studies have shown that in breast cancer, *GLYATL1* was among genes differently expressed in the contralateral unaffected breast in women with estrogen-receptor negative compared to those with estrogen-receptor positive breast cancer (13). In prostate cancer cell lines GLYATL1 was shown to play a role in colony forming ability(14). To date its expression in cancerous tissue and its role in tumorigenesis is not well understood.

In this study we sought to analyze the expression and regulation of GLYATL1 in prostate cancer. Our investigation suggests that GLYATL1 is overexpressed in low grade disease.

Furthermore, we show that androgen treatment and ETS transcription factor ETV1 plays a role in regulating its expression.

2. Materials and Methods

2.1 Gene expression from The Cancer Genome Atlas (TCGA)

Gene expression levels of *GLYATL1* in normal prostate and prostate adenocarcinoma were interrogated utilizing UALCAN (http://ualcan.path.uab.edu), a web portal providing TCGA RNA sequencing data in the form of boxplots, depicting gene expression levels.(15)

2.2 Prostate tissue samples

Benign and prostate cancer tissues were obtained from radical prostatectomy series and from Rapid Autopsy Program at the University of Michigan through appropriate informed consent. Institutional Review Board approval was obtained to procure and analyze the tissues. Two tissue microarrays including 134 patients were constructed with a total of 321 TMA spots.

2.3 Immunohistochemistry (IHC)

IHC was carried out to evaluate GLYATL1 expression using rabbit polyclonal antibody against GLYATL1 (Sigma Aldrich, MO, catalog # HPA039501, 1:200). Formalin-fixed, paraffin-embedded tissue sections were deparaffinized and rehydrated. Antigen retrieval was performed by boiling the slides for 10 minutes in citrate buffer (Sigma Aldrich, MO, catalog #C9999-1000ML). Immunostaining was performed using Vector Laboratories staining kit following the manufacturer's protocol. Endogenous peroxidase activity was blocked using BLOXALL Blocking Solution (Vector Laboratories, catalog #SP-6000). Non-specific binding sites were blocked by incubation with normal horse serum (Vector

Laboratories, R.T.U., 2.5%, catalog #S-2012). Primary antibody was added in a 1:200 dilution for 1 ½ h at room temperature according to dilution protocol optimized in our laboratory. After washing with PBS, secondary antibody (Vector Laboratories, anti-rabbit, catalog #MP-7401) was added for 45 min at room temperature. Following two washings (5min each) with PBS and PBS-T, antibody signals were detected using ImmPACT DAB (Vector laboratories, catalog #SK-4105). Hematoxylin QS (Vector Laboratories, catalog # H-3404) was used as a counterstain. Sections were then dehydrated.

2.4 Immunohistochemical scoring system

GLYATL1 IHC expression was evaluated by a genitourinary pathologist. The scoring system consisted of a modified quantitative H-score system (ranging from 0 to 300) in which GLYATL1 expression was estimated as the products of the intensity (0 for negative, 1 for weakly positive, 2 for moderately positive, and 3 for strongly positive) multiplied by the extent of the staining in the tumor cells (0% to 100%). GLYATL1 score is reported by diagnosis and by Gleason score. Each sample core was plotted with multiple cores per patient. The mean, 95% confidence intervals, and pairwise t-test p-values reported were adjusted for the correlation among multiple samples per patient using a clustered analysis. The analysis for Figure 3 was generated using SAS software. Copyright © 2016 SAS Institute Inc. SAS and all other SAS Institute Inc. product or service names are registered trademarks or trademarks of SAS Institute Inc., Cary, NC, USA.

2.5 Western blot analyses

For Western blot analysis, protein samples were, as previously described,(16) separated on SDS–PAGE (Invitrogen 4-12%). Equal amounts of proteins were loaded and transferred for 2h at 0.35A onto an Immobilon1-P PVDF membrane (EMD Millipore, Billerica, MA). To block non-specific binding, the membrane was incubated for 1 h in blocking buffer (Tris-buffered saline, 0.1% Tween 20 [TBS-T], 5% nonfat dry milk) followed by incubation overnight at 4°C with the primary antibody. After two washes with TBS-T for 5 min, the blot was incubated with horseradish peroxidase-conjugated secondary antibody (1:5000) for 1 h at room temperature. The membrane was again washed with TBS-T and TBS twice for 5 min each and signals were visualized by LuminataTM Crescendo chemiluminescence western blotting substrate as per manufacturer's protocol (EMD Millipore). For loading control β-actin was applied. Therefore the membrane was incubated, after two washes with TBS-T, with the anti-β-actin antibody for 1h at room temperature. After again two washings with TBS-T and TBS signals were visualized, as described above, using LuminataTM Crescendo chemiluminescence western blotting substrate as per manufacturer's protocol (EMD Millipore). Antibodies used in the study are anti-GLYATL1 (Sigma Aldrich, MO, catalog # HPA039501, 1:1000), anti-PSA rabbit polyclonal antibody (Dako, Dako Denmark A/S 1:1000), anti-HRP-β-actin (PTG Labs, Rosemont, IL, catalog # HRP-60008, 1:20000), anti-rabbit IgG HRP (PTG Labs, Rosemont, IL, catalog # SA00001-2, 1:5000). All antibodies were employed at dilutions optimized in our laboratory.

2.6 Cell culture

Human prostate cancer cell lines LNCaP, C4-2B, 22Rv1, PC3, DU145 and VCaP as well as RWPE-1 were obtained from ATCC. LNCaP, C4-2B, 22Rv1, PC3 and DU145 cells were cultivated at 37°C in RPMI medium (Gibco™ RPMI 1640 Medium [+] L-Glutamine , Life Technologies™) supplemented with 10% fetal bovine serum and 100 U/ml penicillin G and 100 µg/ml streptomycin in a humidified environment with 5% CO2. VCaP cells were cultivated at 37°C in Dulbecco's Modified Eagle Medium +GlutaMAX (Gibco™ DMEM(1x) + GlutaMAX™, Life Technologies™) supplemented with 10% fetal bovine serum and 100 U/ml penicillin G and 100 µg/ml streptomycin (Life Technologies™) in a humidified environment with 5% CO2. RWPE-1 cells were cultivated in Keratinocyte Serum Free Medium (Gibco™ Life Technologies) supplemented with 2.5µg EGF (Gibco™ Life Technologies) and 25mg Bovine Pituitary Extract (Life Technologies) and 100 U/ml penicillin G and 100 µg/ml streptomycin (Life Technologies™) in a humidified environment with 5% CO2. Normal prostate epithelial cells (PrEC) were obtained from Clonetics Corporation (San Diego, CA) and were maintained in prostate epithelial cell medium (PrEGM) supplemented with a mixture of various growth factors (SingleQuots) (Clonetics); and 10% fetal bovine serum.

2.7 GLYATL1 and ETV1 knockdown in prostate cancer cells

ETV1 and non-targeting small interfering RNA (siRNA) were obtained from Dharmacon, (Lafayette, CO) and transfection experiments were performed followed the manufacture's protocol. For transfection Lipofectamine RNAiMAX reagent (Thermo Fisher) was applied. Cells were seeded 1 x 10^5 in a 6-well plate and simultaneously transfected with siRNA. Twenty-four hours later a second identical transfection was performed. Cells

were harvested 72h after the first transfection for RNA isolations and Western blot experiments. siRNA used in this study are shown in Supplementary Table T1.

Stable knockdowns were created using shRNA purchased from SBI (System Biosciences, Mountain View, CA, see Supplementary Table T2.). Lentiviruses for creating these stable knockdowns were created by the University of Alabama at Birmingham Vector Core. After infection of prostate cells with lentiviruses expressing GLYATL1 shRNA or non-targeting shRNA, stable knockdown cell lines were generated by selection with 1µg/ml puromycin (Life Technologies).

2.8 RNA extraction and Real-time PCR (RT-PCR)

Total RNA from prostate cancer cells was extracted by using Direct-zol RNA MiniPrep Plus kit (Zymo Research) according to manufacturer's protocol. RNA from tissue was harvested by employing the Qiagen RNAeasy kit. Each sample was transcribed into cDNA by using Superscript III Reverse Transcriptase (ThermoFischer Scientific), deoxynucleoside triphosphates, and random hexamer primers (ThermoFischer Scientific). For each RT-PCR amplification, 2µl of cDNA (200ng/µl) product, 5 µl SYBR green PCR Master Mix (Applied Biosystems), 1 µl primer solution, and 2 µl of DNAse/RNAse free water was added for a final volume of 10µl. Thermocylcling conditions were as suggested by the manufacturer: 95° for 20 sec to activate the polymerase followed by 40 cycles of 95° for 15 sec and 60° for 1 min. SYBR green was used to determine the mRNA expression level of a gene of interest. Levels were normalized to beta-Actin using the ΔΔCT method. All primers for SYBR green were synthesized by Integrated DNA Technologies (Coralville, IA) and listed in Supplementary Table T3. All PCRs were performed in triplicates.

2.9 Transcriptome sequencing analyses.

RNA from prostate cancer cells (22Rv1 and LNCaP) treated with GLYATL1 shRNA and non-targeting shRNA were sequenced using Illumina sequencer. The raw sequence reads obtained as FASTQ files were trimmed using Trim Galore (v0.4.1) [http://www.bioinformatics.babraham.ac.uk/projects/trim_galore/] to remove adapter sequences and low quality reads. After performing the quality control analysis using FastQC (v0.11.5) [http://www.bioinformatics.babraham.ac.uk/projects/fastqc/], the trimmed reads were mapped to human genome (GRCh38/hg38) using TopHat v2.1.0 (17). The aligned reads were sorted via samtools (Version: 1.3.1).(18) HTSeq-count (version 0.6.0)(19) was used to obtain raw read counts for each annotated human gene. Differential expression analysis between GLYATL1 shRNA and non-targeting shRNA treated samples was carried out using DESeq (20) considering "blind" method for estimating dispersion and "fit-only" sharing mode. Genes with absolute fold change of 1.5 or more and p-value <0.05 were considered as differentially expressed [DEG]. Gene ontology and Kyoto Encyclopedia of Genes and Genomes (KEGG) pathway enrichment analysis on differentially expressed genes were performed using online platform DAVID (Database for Annotation, Visualization and Integrated Discovery) version 6.8.(21) Volcano plots and heatmap were generated in R 3.2.2 (https://cran.r-project.org/) using gplots package [https://cran.r-project.org/web/packages/gplots/index.html].

2.10 Accession numbers

The RNA sequencing data are submitted to the Gene Expression Omnibus (GEO) database, www.ncbi.nlm.nih.gov/geo (accession no. GSE130395)

2.11 ChIP sequencing and promoter analyses

AR binding in the *GLYATL1* promoter region in prostate cancer cells (LNCaP) treated with dihydrotestosterone (DHT) was explored. SRA files corresponding to GSE83860 (22) and GSE92347 (23) were downloaded. Supplementary Table 4 shows complete list of raw data downloaded and processed. Downloaded SRA files were converted to FASTQ files using SRA Toolkit (https://www.ncbi.nlm.nih.gov/sra/docs/toolkitsoft/). ChIP-seq raw data were processed as mentioned in Chakravarthi et al.(24) The upstream region of GLYATL1 and KLK3 (as positive control) was explored for AR binding using Integrative Genome Viewer (IGV).(25)

AR peak sequence located within *GLYATL1* promoter region was extracted, and scanned for AR position weight matrix [PWM] (MA0007.2) using JASPAR database.(26) Details of AR ChIP-seq raw data files downloaded from NCBI Sequence Read Archive (SRA) database are shown in Supplementary Table T4.

2.12 Statistical Analysis

GLYATL1 expression index (EI) from tissue microarrays was reported by tissue diagnosis and Gleason score separately. Expression index equals the intensity expression score multiplied by the percent of cells displaying the expression. Each sample core was plotted with multiple cores per patient. The mean, 95% confidence intervals, and pairwise t-test p-values reported were adjusted for the correlation among multiple samples per patient using a clustered analysis. The statistical analysis of the tissue microarray immunohistochemistry data was generated using SAS software. Copyright © 2016 SAS Institute Inc. SAS and all other SAS Institute Inc. product or service names are registered trademarks or trademarks of SAS Institute Inc., Cary, NC, USA.

Statistical analysis for cell proliferation study was performed by using JMP® 13.1.0. To determine significant differences between two groups, the Wilcoxon rank sum test was applied for continuous variables. P values <0.05 were considered significant.

3. Results

3.1 *GLYATL1* is overexpressed in low grade and localized prostate cancer

Based on our *in silico* analysis of publicly available prostate cancer gene expression data using the Oncomine database [OncomineTM Platform] (Life Technologies, Ann Arbor, MI](27) we found *GLYATL1* to be overexpressed in human prostate adenocarcinomas in seven independent gene expression profiling studies (Figure 1A) (p=1.78E-5).(28-33) By applying the Oncomine data base and the web portal UALCAN (15) it could be shown that *GLYATL1* was significantly overexpressed in human prostate cancer compared to benign prostate tissue in the study by Lapointe et al.(31) (See Supplementary Figure 1A) and the TCGA study cohort(2) (p =1.624E-12) (Figure 1B). The *in silico* analysis of the study by Grasso et al. revealed an overexpression of *GLYATL1* in primary prostate cancer compared to benign tissue and metastatic tumors (Figure 1C). Furthermore, *GLYATL1* was especially overexpressed in the lower grade tumors in the TCGA study cohort (Figure 1D). Looking at the three other Human Glycine N-acyltransferases (*GLYATL2*, *GLYATL3*, and *GLYAT*) revealed that the observed overexpression in prostate cancer was unique for *GLYATL1* (Figure 1E).

3.2 Immunohistochemical and Western Blot analyses of GLYATL1 in prostate cancer tissue

Using a GLYATL1 specific antibody, we performed immunohistochemistry staining on TMAs containing benign prostatic tissue, prostatic intraepithelial neoplasia (PIN), localized and metastatic prostate cancer. Representative staining patterns are depicted in Figure 2. The arrow in the Fig. 2F shows the prostate cancer liver metastasis showing absence of GLYATL1 expression. TMA analyses showed an increased GLYATL1 protein expression in line with our *in silico* analysis of GLYATL1 mRNA. GLYATL1 is overexpressed especially in localized prostate tumors compared to normal prostatic tissue ($p<.0001$), PIN ($<.0001$) and metastatic prostate cancer ($p<.0001$) (Figure 3 A and B). Analyses of a subset of prostatic adenocarcinomas based on grade showed a higher GLYATL1 expression in Gleason score 5, 6, and 7 tumors compared to those with Gleason score 8 and 9. Furthermore, Western Blot experiments revealed that GLYATL1 protein was present primarily in localized prostate cancer and metastases, and it was not detectable in benign tissue (Figure 3C).

3.3 GLYATL1 expression is regulated by androgen and ETV1

RT-PCR (Figure 4A) and Western blot analysis (Figure 4B) displayed that GLYATL1 is expressed in the androgen receptor (AR) containing prostate cancer cell lines LNCaP, C4-2B, 22Rv1, and VCaP. It was absent in prostate epithelial cells and RWPE-1 (resembling cells of benign prostatic hyperplasia), as well as PC3 and DU145, which lack androgen receptor expression. After treating LNCaP with 5 nM Methyltrienolone (R1881) and 10nM DHT for 48 hours, levels of GLYATL1 mRNA were increased compared to GLYATL1 levels in non-treated or vehicle-control cells (Figure 4C).

Similarly, mRNA expression levels of the androgen regulated gene prostate specific antigen (PSA) were increased (Figure 4D). Western blot analysis showed similar results (Figure 4E). Analyses of AR ChIP-seq data in DHT treated LNCaP revealed AR occupancy in the *GLYATL1* promoter region (Figure 4F, Supplementary Figure 2B), indicating GLYATL1 as an AR target. Furthermore, GLYATL1 was decreased upon ETV1 knockdown in LNCaP cells (Figure 4G).

3.4 Molecular pathways altered by GLYATL1 modulation in prostate cancer cells

In order to investigate the signaling events that is regulated by GLYATL1, we performed GLYATL1 knockdown using a specific shRNA targeting *GLYATL1* in prostate cancer cell lines LNCaP and 22Rv1. The knockdown in LNCaP was confirmed by RT-PCR and Western blot (Figure 5A). Transcriptome sequencing was performed using RNA from GLYATL1 knockdown (GLYATL1 shRNA) as well as control cells. Figure 5B shows the top 40 up- and down-regulated genes upon GLYATL1 knockdown in LNCaP cells. Our analysis identified that upon GLYALT1 knockdown, 164 protein coding genes were down-regulated and 105 protein coding genes were up-regulated (Figure 5C). Supplementary table 5 and 6 provide the up and down regulated genes in 22Rv1 and LNCaP cells after GLYATL1 knockdown. Supplementary table 7 and 8 provide the biological processes and KEGG pathways altered upon GLYATL1 knockdown in these cells. KEGG pathways enriched in differentially expressed genes on GLYATL1 knockdown includes glycolysis and gluconeogenesis as well Hypoxia-inducible factor 1(HIF-1) signaling, metabolic pathways and central carbon metabolism in cancer (Figure 5D).

Knockdown confirmation, top up-and down-regulated genes, as well as KEGG pathways enriched after GLYATL1 knockdown in 22Rv1 are shown in Supplementary Figure 1B-D.

4. Discussion

In this study, we evaluated the expression and regulation of Glycine-N-Acyltransferase Like 1 in prostate cancer. GLYATL1 as an enzyme, involved in N-acyl amino acid production and metabolism, is normally expressed in liver and kidney.(6,7) Microarray studies have shown its overexpression in prostate cancer.(5,14,34,35) Our *in silico* analysis further indicates, GLYATL1 transcripts to be higher in localized prostate cancers compared to benign prostatic tissue and metastatic prostate cancer. Especially the lower Gleason grade tumors (≤7) showed a high GLYATL1 expression. This was further confirmed by Western blot analysis and immunohistochemistry, showing GLYATL1 protein expression to be low in benign prostate tissue, PIN and most of the metastatic prostate cancers.

To evaluate the potential role of GLYATL1 in prostate cancer, we analyzed its expression in prostate cancer cell lines. In their study on next generation RNAseq in castration-resistant prostate cancer cell lines, Ma et al. found *GLYATL1* among the top 8 down-regulated genes in PC3 and DU145 (which represent acquired resistance to androgens) vs. LNCaP cells.(36) In line with that, we found GLYATL1 to be present in prostate cancer cell lines that express AR (LNCaP, C4-2B, VCaP and 22Rv1) and absent in DU145, PC3, benign prostate epithelial cells and RWPE-1. Our analyses further identified that GLYATL1 expression is induced by androgen treatment in LNCaP cells.

ChIP-Seq data analyses showed AR binding in the promoter region of the *GLYATL1* gene, emphasizing a direct regulation of GLYATL1 by androgen signaling. As prostate cancer growth is initially androgen dependent, the gold-standard treatment option for advanced disease is androgen deprivation.(37) However, most patients eventually develop resistance and disease progression. Thus, several studies have investigated signaling events that lead to castration-resistant prostate cancer (CRPC). (30,38,39) Kaushik et al. have recently shown, that glucosamine-phosphate N-acetyltransferase 1, an enzyme involved in the hexosamine biosynthetic pathway, is significantly decreased in CRPC compared to localized prostate cancer.(38) Similarly, we found GLYATL1 to be lower in metastatic prostate cancer. Whether this expression pattern has a role for GLYATL1 in the development of CRPC remains to be investigated.

As mentioned above, chromosomal rearrangements involving ETS transcription factors, such as ERG and ETV1, are the most frequent alterations in prostate cancer. Translocations place the coding regions of the latter mentioned genes under the control of androgen-responsive promoters, such as *TMPRSS2*. (40) ETV1 expression in ETV1 knock-in mice was found to positively cooperate with AR signaling, leading to additional enhancement of expression of AR targets.(41) In line with this mechanism, we found GLYATL1 not only to be upregulated upon androgen treatment, but also down regulated in LNCaP cells following ETV1 knockdown, indicating a potential regulatory role for this ETS transcription factor in GLYATL1 expression.

Serum level of prostate-specific antigen (PSA) is a widely used screening biomarker.(42) However, PSA elevation is not very specific for prostate cancer, as numerous benign conditions, like benign prostatic hyperplasia, can cause a rise in its

serum levels. Therefore, there is a need for additional risk stratification. In this setting, urine as a liquid biopsy platform is actively being investigated. In a study by Leyten et al. *GLYATL1*, along with 15 other biomarkers, was described to be differentially expressed in urine sediments from prostate cancer patients compared to healthy controls.(35) This further emphasizes GLYATL1's potential as an early stage biomarker.

In order to understand the pathways that may be regulated by GLYATL1, we performed RNA sequencing using shRNA specifically targeting GLYATL1 in prostate cancer cell lines. Pathway analysis in LNCaP GLYATL1 knockdown cells revealed a potential involvement in metabolic pathways including glycolysis. Anaerobic glycolysis has been shown to be one of the main metabolic changes in CRPC-like cells.(43) Whether GLYATL1 knockdown could be similarly implicated in driving LNCaP cells towards a more aggressive phenotype will require further assessment and could then provide a rational for our finding of lower GLYATL1 levels in metastatic tumors compared to localized prostate cancers.

In summary, our study further characterizes the expression GLYATL1 in prostate cancer and explores its regulation. We show GLYATL1 overexpression mainly in low grade and localized prostate cancer. Additionally, our findings indicate that androgen and ETV1 are involved in its regulation. Future studies are needed to decipher the biological significance of these findings.

Acknowledgement

We thank the University of Alabama at Birmingham Vector Core for generating lentiviruses and the Genomics Core Laboratories.

Conflicts of interest

No potential conflicts of interest were disclosed.

References

1. Siegel RL, Miller KD, Jemal A. Cancer statistics, 2019. CA Cancer J Clin 2019;69(1):7-34.

2. Network CGAR. The Molecular Taxonomy of Primary Prostate Cancer. Cell 2015;163:1011-1025.

3. Chakravarthi BV, Nepal S, Varambally S. Genomic and Epigenomic Alterations in Cancer. Am J Pathol 2016;186(7):1724-1735.

4. Matsuo M, Terai K, Kameda N, Matsumoto A, Kurokawa Y, Funase Y, Nishikawa K, Sugaya N, Hiruta N, Kishimoto T. Designation of enzyme activity of glycine-N-acyltransferase family genes and depression of glycine-N-acyltransferase in human hepatocellular carcinoma. Biochem Biophys Res Commun 2012;420(4):901-906.

5. Barfeld SJ, East P, Zuber V, Mills IG. Meta-analysis of prostate cancer gene expression data identifies a novel discriminatory signature enriched for glycosylating enzymes. BMC Med Genomics 2014;7:513.

6. Zhang H, Lang Q, Li J, Zhong Z, Xie F, Ye G, Wan B, Yu L. Molecular Cloning and Characterization of a Novel Human Glycine-N-acyltransferase Gene GLYATL1, Which Activates Transcriptional Activity of HSE Pathway. International Journal of Molecular Sciences 2007.

7. van der Sluis R, Badenhorst CP, Erasmus E, van Dyk E, van der Westhuizen FH, van Dijk AA. Conservation of the coding regions of the glycine N-acyltransferase gene further suggests that glycine conjugation is an essential detoxification pathway. Gene 2015;571(1):126-134.

8. Badenhorst CP, Erasmus E, van der Sluis R, Nortje C, van Dijk AA. A new perspective on the importance of glycine conjugation in the metabolism of aromatic acids. Drug Metab Rev 2014;46(3):343-361.

9. Badenhorst CPS, van der Sluis R, Erasmus E, van Dijk AA. Glycine conjugation: importance in metabolism, the role of glycine N-acyltransferase, and factors that influence interindividual variation. Expert Opinion on Drug Metabolism & Toxicology 2013;9(9):1139-1153.

10. Waluk DP, Sucharski F, Sipos L, Silberring J, Hunt MC. Reversible lysine acetylation regulates activity of human glycine N-acyltransferase-like 2

(hGLYATL2): implications for production of glycine-conjugated signaling molecules. J Biol Chem 2012;287(20):16158-16167.

11. Paulo P, Ribeiro FR, Santos J, Mesquita D, Almeida M, Barros-Silva JD, Itkonen H, Henrique R, Jeronimo C, Sveen A, Mills IG, Skotheim RI, Lothe RA, Teixeira MR. Molecular subtyping of primary prostate cancer reveals specific and shared target genes of different ETS rearrangements. Neoplasia 2012;14(7):600-611.

12. Tomlins SA, Rhodes DR, Perner S, Dhanasekaran SM, Mehra R, Sun X-W, Varambally S, Cao X, Tchinda J, Kuefer R, Lee C, Montie JE, Shah RB, Pienta KJ, Rubin MA, Chinnaiyan AM. Recurrent fusion of TMPRSS2 and ETS transcription factor genes in prostate cancer. Science (New York, NY) 2005;310:644-648.

13. Wang J, Shidfar A, Ivancic D, Ranjan M, Liu L, Choi MR, Parimi V, Gursel DB, Sullivan ME, Najor MS, Abukhdeir AM, Scholtens D, Khan SA. Overexpression of lipid metabolism genes and PBX1 in the contralateral breasts of women with estrogen receptor-negative breast cancer. Int J Cancer 2017;140(11):2484-2497.

14. Nalla AK, Williams TF, Collins CP, Rae DT, Trobridge GD. Lentiviral vector-mediated insertional mutagenesis screen identifies genes that influence androgen independent prostate cancer progression and predict clinical outcome. Mol Carcinog 2016;55(11):1761-1771.

15. Chandrashekar DS, Bashel B, Balasubramanya SAH, Creighton CJ, Ponce-Rodriguez I, Chakravarthi BVSK, Varambally S. UALCAN: A Portal for Facilitating Tumor Subgroup Gene Expression and Survival Analyses. Neoplasia (New York, NY) 2017;19:649-658.

16. Chakravarthi BV, Goswami MT, Pathi SS, Dodson M, Chandrashekar DS, Agarwal S, Nepal S, Hodigere Balasubramanya SA, Siddiqui J, Lonigro RJ, Chinnaiyan AM, Kunju LP, Palanisamy N, Varambally S. Expression and Role of PAICS, a De Novo Purine Biosynthetic Gene in Prostate Cancer. Prostate 2017;77(1):10-21.

17. Kim D, Pertea G, Trapnell C, Pimentel H, Kelley R, Salzberg SL. TopHat2: accurate alignment of transcriptomes in the presence of insertions, deletions and gene fusions. Genome Biol 2013;14(4):R36.

18. Li H. A statistical framework for SNP calling, mutation discovery, association mapping and population genetical parameter estimation from sequencing data. Bioinformatics 2011;27(21):2987-2993.

19. Anders S, Pyl PT, Huber W. HTSeq--a Python framework to work with high-throughput sequencing data. Bioinformatics 2015;31(2):166-169.

20. Anders S, Huber W. Differential expression analysis for sequence count data. Genome Biol 2010;11(10):R106.

21. Huang da W, Sherman BT, Lempicki RA. Systematic and integrative analysis of large gene lists using DAVID bioinformatics resources. Nat Protoc 2009;4(1):44-57.

22. Malinen M, Niskanen EA, Kaikkonen MU, Palvimo JJ. Crosstalk between androgen and pro-inflammatory signaling remodels androgen receptor and NF-kappaB cistrome to reprogram the prostate cancer cell transcriptome. Nucleic Acids Res 2017;45(2):619-630.

23. Chattopadhyay I, Wang J, Qin M, Gao L, Holtz R, Vessella RL, Leach RW, Gelman IH. Src promotes castration-recurrent prostate cancer through androgen receptor-dependent canonical and non-canonical transcriptional signatures. Oncotarget 2017;8(6):10324-10347.

24. Chakravarthi B, Chandrashekar DS, Hodigere Balasubramanya SA, Robinson AD, Carskadon S, Rao U, Gordetsky J, Manne U, Netto GJ, Sudarshan S, Palanisamy N, Varambally S. Wnt receptor Frizzled 8 is a target of ERG in prostate cancer. Prostate 2018;78(16):1311-1320.

25. Robinson JT, Thorvaldsdottir H, Winckler W, Guttman M, Lander ES, Getz G, Mesirov JP. Integrative genomics viewer. Nat Biotechnol 2011;29(1):24-26.

26. Khan A, Fornes O, Stigliani A, Gheorghe M, Castro-Mondragon JA, van der Lee R, Bessy A, Cheneby J, Kulkarni SR, Tan G, Baranasic D, Arenillas DJ, Sandelin A, Vandepoele K, Lenhard B, Ballester B, Wasserman WW, Parcy F, Mathelier A. JASPAR 2018: update of the open-access database of transcription factor binding profiles and its web framework. Nucleic Acids Res 2018;46(D1):D260-D266.

27. Rhodes DR, Kalyana-Sundaram S, Mahavisno V, Varambally R, Yu J, Briggs BB, Barrette TR, Anstet MJ, Kincead-Beal C, Kulkarni P, Varambally S, Ghosh D, Chinnaiyan AM. Oncomine 3.0: genes, pathways, and networks in a collection of 18,000 cancer gene expression profiles. Neoplasia 2007;9(2):166-180.

28. Varambally S, Yu J, Laxman B, Rhodes DR, Mehra R, Tomlins SA, Shah RB, Chandran U, Monzon FA, Becich MJ, Wei JT, Pienta KJ, Ghosh D, Rubin MA, Chinnaiyan AM. Integrative genomic and proteomic analysis of prostate cancer reveals signatures of metastatic progression. Cancer Cell 2005;8(5):393-406.

29. Arredouani MS, Lu B, Bhasin M, Eljanne M, Yue W, Mosquera JM, Bubley GJ, Li V, Rubin MA, Libermann TA, Sanda MG. Identification of the transcription factor single-minded homologue 2 as a potential biomarker and immunotherapy target in prostate cancer. Clin Cancer Res 2009;15(18):5794-5802.

30. Grasso CS, Wu Y-M, Robinson DR, Cao X, Dhanasekaran SM, Khan AP, Quist MJ, Jing X, Lonigro RJ, Brenner JC, Asangani IA, Ateeq B, Chun SY, Siddiqui J, Sam L, Anstett M, Mehra R, Prensner JR, Palanisamy N, Ryslik GA, Vandin F, Raphael BJ, Kunju LP, Rhodes DR, Pienta KJ, Chinnaiyan AM, Tomlins SA. The

mutational landscape of lethal castration-resistant prostate cancer. Nature 2012;487:239-243.

31. Lapointe J, Li C, Higgins JP, van de Rijn M, Bair E, Montgomery K, Ferrari M, Egevad L, Rayford W, Bergerheim U, Ekman P, DeMarzo AM, Tibshirani R, Botstein D, Brown PO, Brooks JD, Pollack JR. Gene expression profiling identifies clinically relevant subtypes of prostate cancer. Proceedings of the National Academy of Sciences of the United States of America 2004;101:811-816.

32. Taylor BS, Schultz N, Hieronymus H, Gopalan A, Xiao Y, Carver BS, Arora VK, Kaushik P, Cerami E, Reva B, Antipin Y, Mitsiades N, Landers T, Dolgalev I, Major JE, Wilson M, Socci ND, Lash AE, Heguy A, Eastham JA, Scher HI, Reuter VE, Scardino PT, Sander C, Sawyers CL, Gerald WL. Integrative genomic profiling of human prostate cancer. Cancer Cell 2010;18:11-22.

33. Vanaja DK, Cheville JC, Iturria SJ, Young CY. Transcriptional silencing of zinc finger protein 185 identified by expression profiling is associated with prostate cancer progression. Cancer Res 2003;63(14):3877-3882.

34. Arencibia JM, Martin S, Perez-Rodriguez FJ, Bonnin A. Gene expression profiling reveals overexpression of TSPAN13 in prostate cancer. Int J Oncol 2009;34(2):457-463.

35. Leyten GH, Hessels D, Smit FP, Jannink SA, de Jong H, Melchers WJ, Cornel EB, de Reijke TM, Vergunst H, Kil P, Knipscheer BC, Hulsbergen-van de Kaa CA, Mulders PF, van Oort IM, Schalken JA. Identification of a Candidate Gene Panel for the Early Diagnosis of Prostate Cancer. Clin Cancer Res 2015;21(13):3061-3070.

36. Ma Y, Miao Y, Peng Z, Sandgren J, De Stahl TD, Huss M, Lennartsson L, Liu Y, Nister M, Nilsson S, Li C. Identification of mutations, gene expression changes and fusion transcripts by whole transcriptome RNAseq in docetaxel resistant prostate cancer cells. Springerplus 2016;5(1):1861.

37. Network NCC. National Comprehensive Cancer Network (NCCN): Prostate Cancer. 2018.

38. Kaushik AK, Shojaie A, Panzitt K, Sonavane R, Venghatakrishnan H, Manikkam M, Zaslavsky A, Putluri V, Vasu VT, Zhang Y, Khan AS, Lloyd S, Szafran AT, Dasgupta S, Bader DA, Stossi F, Li H, Samanta S, Cao X, Tsouko E, Huang S, Frigo DE, Chan L, Edwards DP, Kaipparettu BA, Mitsiades N, Weigel NL, Mancini M, McGuire SE, Mehra R, Ittmann MM, Chinnaiyan AM, Putluri N, Palapattu GS, Michailidis G, Sreekumar A. Inhibition of the hexosamine biosynthetic pathway promotes castration-resistant prostate cancer. Nat Commun 2016;7:11612.

39. Waltering KK, Urbanucci A, Visakorpi T. Androgen receptor (AR) aberrations in castration-resistant prostate cancer. Mol Cell Endocrinol 2012;360(1-2):38-43.

40. Tomlins SA, Mehra R, Rhodes DR, Cao X, Wang L, Dhanasekaran SM, Kalyana-Sundaram S, Wei JT, Rubin MA, Pienta KJ, Shah RB, Chinnaiyan AM. Integrative molecular concept modeling of prostate cancer progression. Nature genetics 2007;39(1):41-51.

41. Baena E, Shao Z, Linn DE, Glass K, Hamblen MJ, Fujiwara Y, Kim J, Nguyen M, Zhang X, Godinho FJ, Bronson RT, Mucci LA, Loda M, Yuan GC, Orkin SH, Li Z. ETV1 directs androgen metabolism and confers aggressive prostate cancer in targeted mice and patients. Genes Dev 2013;27(6):683-698.

42. Schroder FH, Hugosson J, Roobol MJ, Tammela TL, Zappa M, Nelen V, Kwiatkowski M, Lujan M, Maattanen L, Lilja H, Denis LJ, Recker F, Paez A, Bangma CH, Carlsson S, Puliti D, Villers A, Rebillard X, Hakama M, Stenman UH, Kujala P, Taari K, Aus G, Huber A, van der Kwast TH, van Schaik RH, de Koning HJ, Moss SM, Auvinen A, Investigators E. Screening and prostate cancer mortality: results of the European Randomised Study of Screening for Prostate Cancer (ERSPC) at 13 years of follow-up. Lancet 2014;384(9959):2027-2035.

43. Shafi AA, Putluri V, Arnold JM, Tsouko E, Maity S, Roberts JM, Coarfa C, Frigo DE, Putluri N, Sreekumar A, Weigel NL. Differential regulation of metabolic pathways by androgen receptor (AR) and its constitutively active splice variant, AR-V7, in prostate cancer cells. Oncotarget 2015;6(31):31997-32012.

Figures

Figure 1. The human N-acytransferase GLYATL1 shows increased expression in prostate cancer. (A) Gene expression profiling analysis of multiple prostate cancer datasets using Oncomine database shows higher GLYATL1 expression in primary prostate cancer compared to benign prostate tissue across the datasets (The rank for a gene is the median rank for that gene across each of the analyses. The Pvalue for a gene is its Pvalue for the medianranked analysis.). (B) Transcriptome sequencing of prostate cancer. GLYATL1 expression in benign, primary, and metastatic prostate cancer were measured in transcript per million utilizing the TCGA dataset. (C) Expression of GLYATL1 in normal prostate, primary and metastatic tumor samples using the Dataset by Grasso et al. (D) GLYATL1 expression analysis per Gleason score utilizing the TCGA dataset. (E) Expression of the human Glycine N-acyltransferases (GLYATL1, GLYATL2, GLYATL3, GLYAT) in primary prostate cancer and normal prostate tissue.

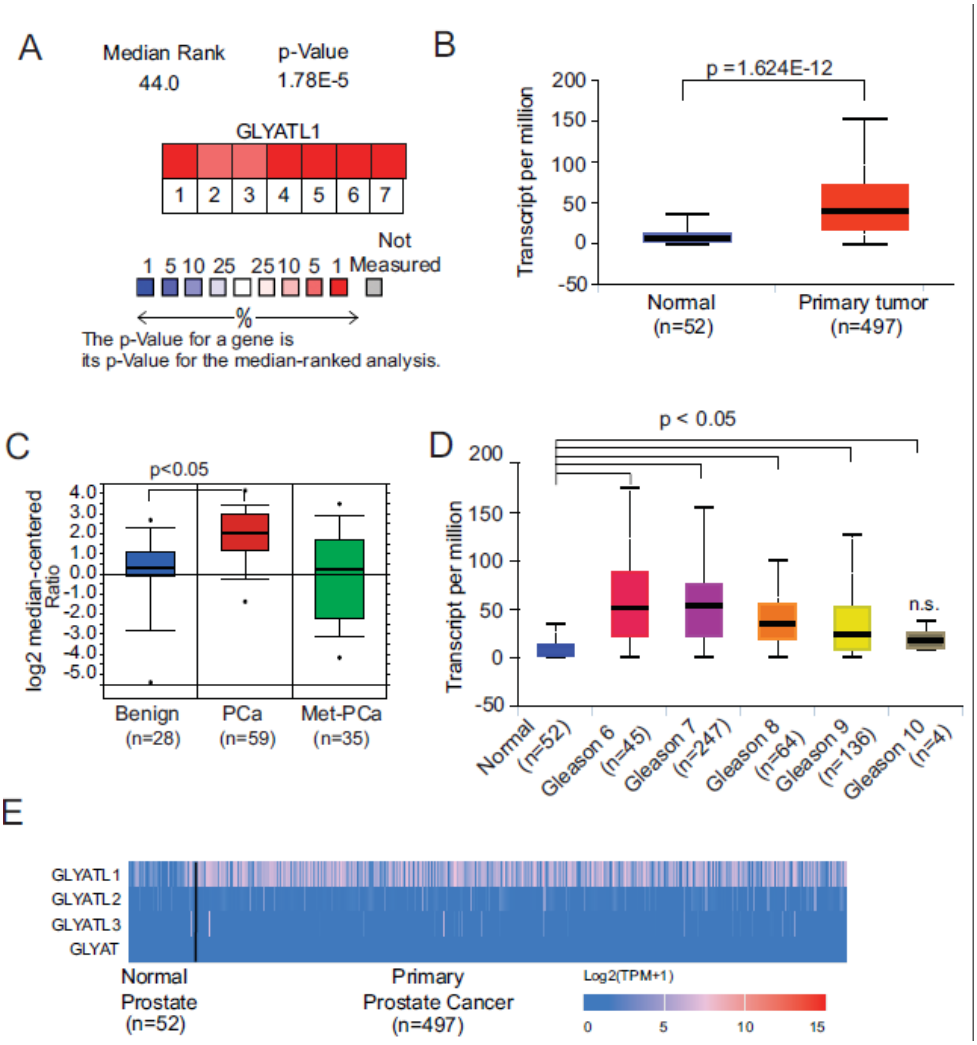

Figure 2. Immunohistochemical staining of GLYATL1 in prostate. (A) benign prostate tissue, (B) high-grade prostatic intraepithelial neoplasia (C, D) Gleason score 6 prostate cancer (E) Gleason score 8 prostate cancer (F) liver metastasis of prostate cancer (arrow) showing low or no staining of GLYATL1 Scale bars: 50μm in (A, B, C, E and F). 20μm in (D).

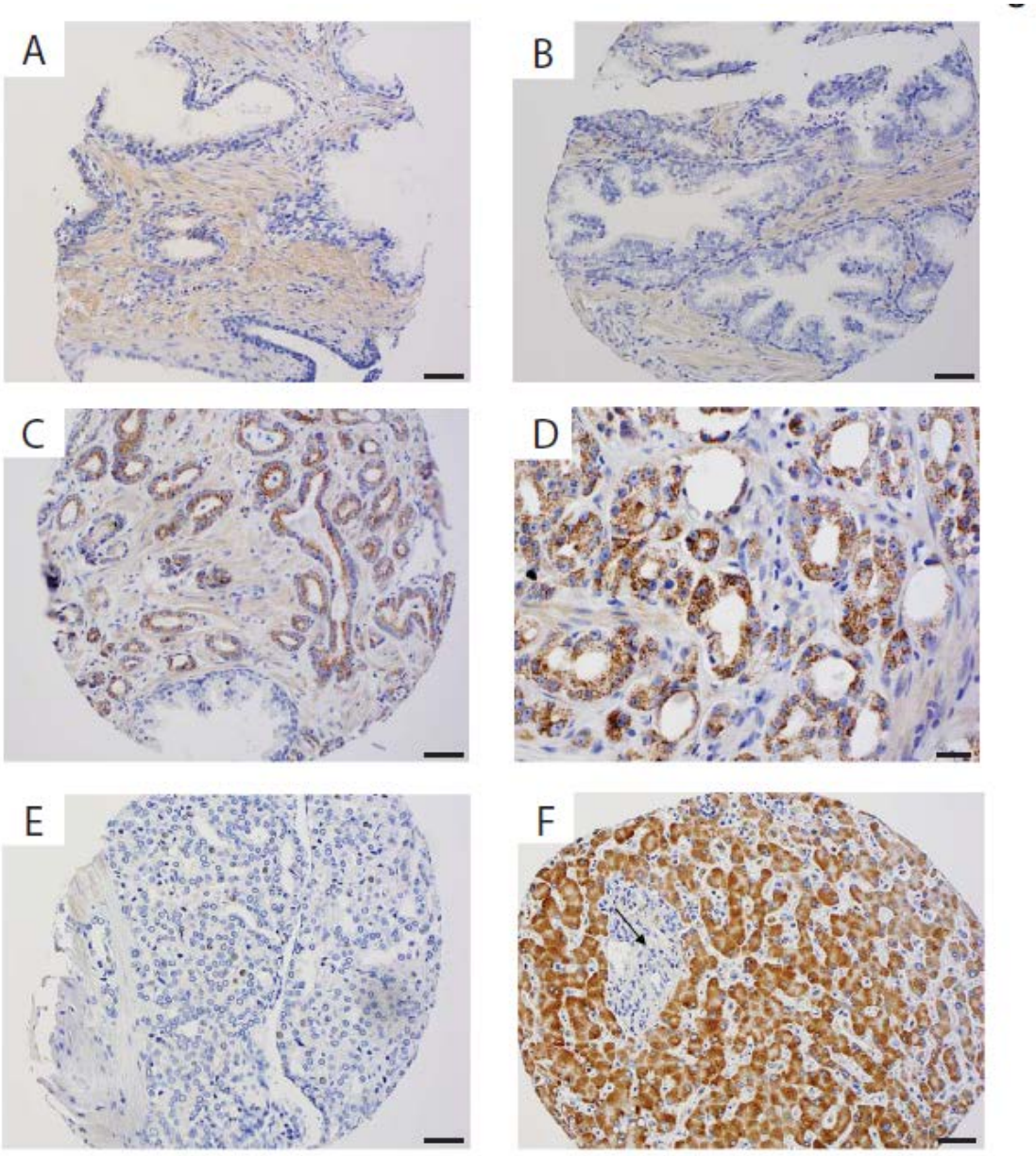

Figure 3. Higher expression of GLYATL1 in primary prostate cancer. (A) immunohistochemical score of GLYATL1 in benign prostate tissue, high-grade prostatic intraepithelial (PIN), primary tumors and metastasis. (B) analysis of GLYATL1 immunohistochemical score in primary prostate cancer per Gleason score. (C) Western Blot analysis of GLYATL1 using benign prostate tissue, primary and metastatic prostate cancer samples.

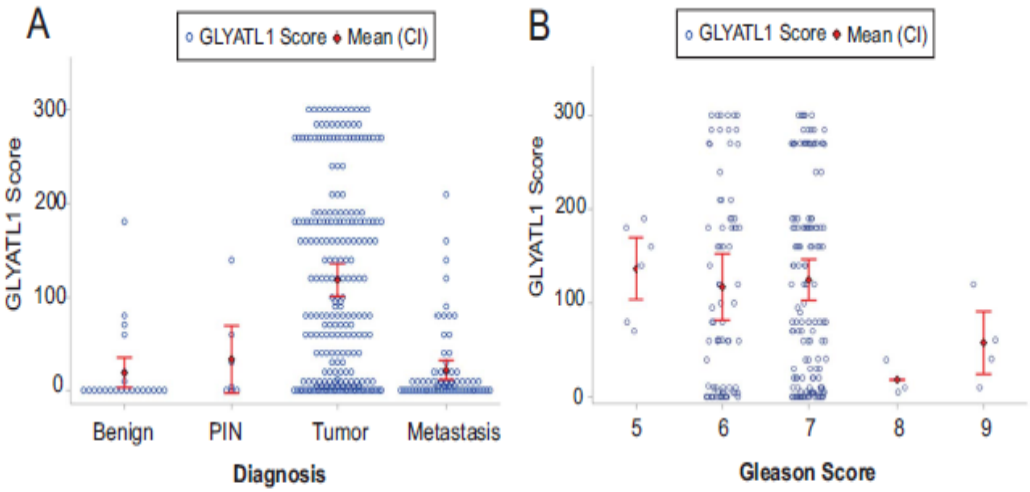

Diagnosis	N	Mean	95% CI for Mean		Comparison to Tumor p-value
Benign	22	19.1	2.9	35.3	<0.0001
PIN	7	33.4	-2.8	69.6	<0.0001
Tumor	236	118.0	100.2	135.9	
Metastasis	70	22.1	11.6	32.6	<0.0001

Gleason Score	N	Mean	95% CI for Mean		Vs 6	Vs 7	Vs 8	Vs 9
5	6	136.7	103.7	169.6	0.43	0.56	<0.0001	0.0013
6	77	117.1	81.3	153.0	--	0.72	<0.0001	0.0188
7	138	124.8	102.5	147.1		--	<0.0001	0.0014
8	3	18.3	18.3	18.3			--	0.0239
9	4	57.5	24.0	91.0				--

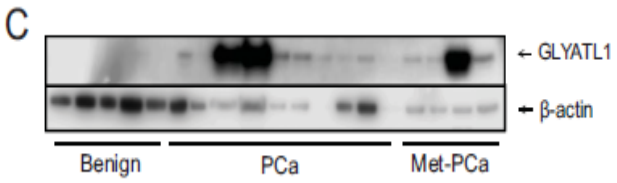

Figure 4. GLYATL1 expression is regulated by androgen and ETV1. (A, B) Western Blot and quantitative reverse transcription PCR analysis of GLYATL1 in prostate cancer cell lines. (C, D) GLYATL1 and prostate-specific antigen (PSA) mRNA expression in untreated, vehicle control treated (ethanol [ETOH]), and androgen treated (dihydrotestosterone [DHT], Methyltrienolone [R1881]) LNCaP cells. (E) Western Blot analysis of GLYATL1 in androgen treated LNCaP cells. (F) IGV output representing gene neighborhood region of GLYATL1, showing AR ChIP-seq peaks in proximal promoter region in LNCaP cells treated with dihydrotestosterone. AR ChIP-seq data from

Malinen et al. [GSE83860] were used.[22] Peaks annotated using Homer shown in the top most lane. AR peak sequence (Chr11:58926274-58926649) with AR consensus (highlighted in pink font) shown below. (G) GLYATL1 expression in ETV1 knockdown LNCaP cells.

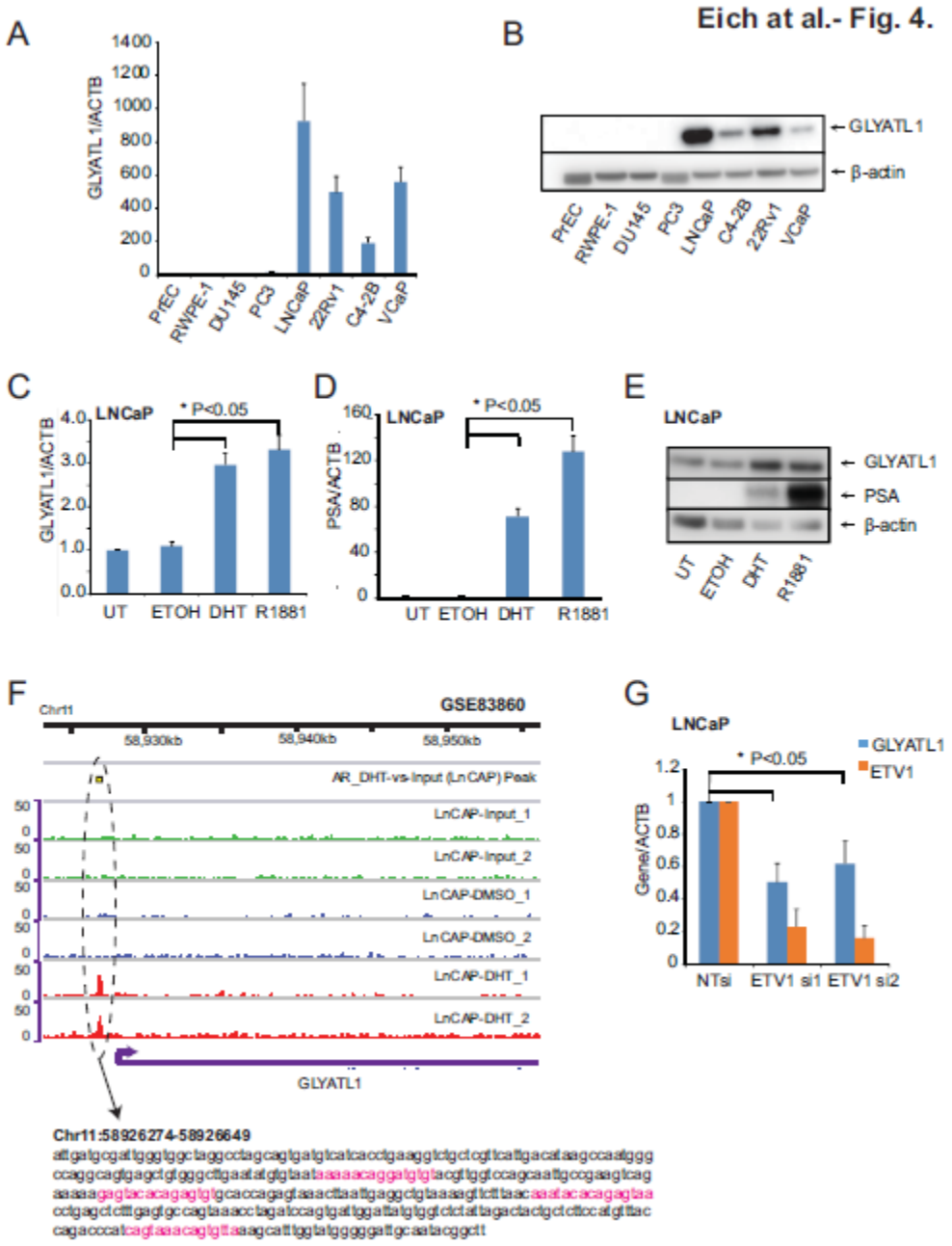

Figure 5. RNA sequencing analysis of GLYATL1 knockdown in LNCaP cells. (A) Western Blot and RT-PCR confirmation of GLYATL1 knockdown in LNCaP cells. (B) Heatmap showing top 40 up- and down-regulated genes after GLYATL1 knockdown in LNCaP cells. (C) Volcano plot showing distribution of differentially expressed genes on

GLYATL1 knockdown in LNCaP cells. Log2 Fold change is represented in x-axis, while y axis represents –log10 P-value. Gene up-regulated are marked with red dots, while blue dots indicate genes down-regulated. (D) Bar plot showing top 10 KEGG pathways enriched in genes differentially expressed on GLYATL1 knockdown in LNCaP cell line.